

# Preparation and Characterization of Nano-hydroxyapatite/polyvinyl Alcohol Gel Composites

PAN Yusong<sup>1</sup>, XIONG Dangsheng<sup>2</sup>

(1. Department of Material Science & Engineering, Anhui University of Science and Technology, Huainan 232001, China;

2. Department of Material Science & Engineering, Nanjing University of Science and Technology, Nanjing 210094, China)

**Abstract:** Nano-hydroxyapatite reinforced poly(vinyl alcohol) gel (nano-HA/PVA gel) composites has been proposed as a promising biomaterial, especially used as an articular cartilage repair biomaterial. In this paper, nano-HA/PVA gel composite was prepared by *in situ* synthesis method and incorporation with freeze-thaw cycle process. The microstructure and morphology were investigated by X-ray diffraction, TEM, SEM and FTIR. The results showed that the size of HA particles synthesized in PVA solution was on the nanometer scale. Both the size and crystallinity of HA particles synthesized in PVA solution decreased compared with that of HA synthesized in distilled water. The nano-HA particles were distributed in PVA matrix uniformly due to the effect of PVA solution as a dispersant while low content of HA particles in the composites. On the contrary, with high content of nano-HA particles in the composites, the particles tended to aggregate. The result of FT-IR analysis indicated that the chemical bond between nano-HA particles and PVA matrix existed. The conformation and degree of tacticity of PVA molecule changed because of the addition of HA particles. Furthermore, the interfacial strength of the composites was improved due to the interaction between nano-HA particle and PVA matrix and this was beneficial to improving the mechanical properties of the composites.

**Key words:** nano-HA/PVA gel composites; freezing-thawing; microstructure; morphology

## 1 Introduction

For various daily activities in human life, tens of millions of people suffer from joint pain caused by the deterioration of articular cartilage, making it a prevalent cause of disability and deteriorating the daily life. Adult articular cartilage has a limited capacity to repair damage resulting from injury or disease. Replacement of articular cartilage is an effective surgical treatment to relieve pain and to restore the locomotion function for patients with damaged joints<sup>[1]</sup>. Recently, there have been many different approaches to restore tissue composition, structure, and function, including the development of engineered cartilage for potential implantation<sup>[2,3]</sup>.

It was found that poly (vinyl alcohol) (PVA) hydrogel is an excellent artificial articular cartilage repair material due to its biocompatibility and biotribological properties<sup>[4-6]</sup>. It possesses high porous structure and high

content of free water, similar to that of natural articular cartilage. PVA hydrogel has increasingly attracted interest in application as an articular repairing material<sup>[7]</sup>. However, it has limited durability and does not adhere well to tissue. For example, for articular cartilage applications PVA may require the use of a fixation method to achieve better adhesion. Furthermore, it is a pendent question to improve the interfacial bonding strength between the implant material and natural tissue<sup>[8]</sup>. Nano-HA has been applied widely in medical field as a bone repair material because of its excellent bioactive properties<sup>[9]</sup>. Nanosized hydroxyapatite particles reinforced PVA gel composites prepared by incorporating Nano-HA with PVA endows composites bioactive properties as well as the improving interfacial bonding strength between nano-HA/PVA composites and natural tissue, because of the implanted material inducing the osteoblast adhesion on and growing into the repair material and thus forming bioactive bonding at the interface. It can also improve interfacial bonding strength and mechanical compatibility between the implanted material and natural tissue. This is the effective method to improve the adhesion properties.

In this paper, nano-HA/PVA gel composites were prepared by *in situ* synthesis of nano-HA particles in PVA solution and combined with freezing-thawing method. The microstructure and morphology of the composite was investigated by XRD, TEM, SEM and FTIR techniques.

## 2 Experimental

### 2.1 Materials

PVA was purchased from Shanghai Chemical Co., Ltd, with the degree of saponification of 99% and number-average degree of polymerization of  $1\ 750 \pm 50$ . For the synthesis of hydroxyapatite,  $\text{Ca}(\text{OH})_2$  (analytical reagent, with purity of 95 wt%) and  $\text{H}_3\text{PO}_4$  (analytical reagent, with purity more than 85 wt%) were supplied by Siopharm Chemical Reagent Co., Ltd. All chemicals were used without any further purification.

### 2.2 Preparation of nano-hydroxyapatite

HA powders were prepared by wet chemical synthesis technique, based on the precipitation of HA particles from aqueous solutions and PVA solution, respectively. The synthesis procedure involved the drop by drop introduction of the  $\text{H}_3\text{PO}_4$  solution (100 mL, 0.6 M) into an aqueous suspension of  $\text{Ca}(\text{OH})_2$  (125 mL, 0.8 M) while stirring vigorously for about 2 h at 80 °C. Ammonia hydroxide solution was added to adjust pH at 10-11. Then the obtained white precipitate was aged for 24 h at 70 °C, decanted, rinsed with deionized water until its pH reached to about 7. After filtration, the precipitate was dried in vacuum oven at 70 °C for 24 h.

### 2.3 Preparation of HA/PVA gel composites

First, 9.3 g  $\text{Ca}(\text{OH})_2$  with purity of 95 wt% was added into the 220 mL distilled water to prepare calcium hydroxide suspension. Second, 77.6 g PVA was introduced into the calcium hydroxide suspension. Third, the blending solution of  $\text{Ca}(\text{OH})_2$  and PVA was stirred continuously at 90 °C for 1 h. Fourth,  $\text{H}_3\text{PO}_4$  solution (90 mL, 0.8 M) was added drop-by-drop to the blending solution of  $\text{Ca}(\text{OH})_2$  and PVA. The solution was maintained thoroughly stirred at 90 °C during the reaction process. The quantities of the reactants were selected to provide a Ca/P molar ratio,  $R$ , of 1.67, such as:

$$R = \frac{n_{\text{Ca}}}{n_{\text{p}}} = 1.67 \quad (1)$$

Where  $n_{\text{Ca}}$  is the number of moles of calcium and  $n_{\text{p}}$  is the number of moles of  $\text{PO}_4^{3-}$ .

After the reaction, the solution was stirred at 90 °C for another 14 h. Subsequently, for degassing of the air trapped in solution during the stirring process, the solu-

tion was stored at 60 °C for 30 min. Then, the mixture was poured into stainless steel container. Finally, the stainless steel container with nano-HA particles and PVA solution were subjected to various cycles of freezing and thawing. In each cycle, the sample was frozen in a commercial freezer regulated at about  $-20$  °C, and allowing it to air cool for about 12 hours. The sample then thawed at room temperature for 6 hours before being returned to the freezer for another cycle. According to this process, different freezing and thawing cycles of nano-HA/PVA gel was prepared.

### 2.4 X-ray diffraction analysis

XRD experiments were performed on HA powder and *n*-HA/PVA gel composites with a diffractometer (2038, REGAKU, Japan), using  $\text{Cu K}\alpha$  radiation ( $\lambda = 1.5406$  Å) at 33 kV and current 15 mA. Samples were scanned over  $2\theta$  range of 15-70° and the step size of scanning is 0.02°.

### 2.5 Microstructure observation

Morphological characterization of the nanometer HAp samples were observed by transmission electron microscopy (TEM) (JEM 2100, JEOL, Japan) after ultrasonic dispersing the dried nano-HAp powder into anhydrous ethanol. The morphology of the nano-HA/PVA gel composites and PVA gel were observed by JSM-6380LV scanning electron microscopy at 20 kV. All the samples were vacuum freeze-dried by vacuum freeze drying machine for 24 h prior to SEM observation.

### 2.6 FTIR spectroscopy

Fourier transform infrared (FTIR) spectroscopy (MB154S, BOMEM, Canada) was used to identify the functional groups of HA powder and *n*-HA/PVA gel composites. A dried sample of 4 mg was carefully mixed with 200 mg of KBr and pressed into a pellet under a hydraulic pressure. The spectrum was recorded in the  $4\ 000\text{-}500\ \text{cm}^{-1}$ . Spectrum analyses were performed using standard Microcal Origin software.

## 3 Results and Discussion

### 3.1 XRD analysis

Fig.1 shows the XRD patterns of the HA power, PVA and *n*-HA/PVA gel composites, respectively. It can be seen from Fig.1(a) that the characteristic peaks of HA were located at 25.86°, 28.98°, 31.86°, 32.26°, 32.98°, 34.1°, 39.94°, 46.74° and 49.48°, respectively. It can be concluded from Fig.1(a) that the XRD peaks of HA diffraction patterns agree well with those of standard HA in the powder diffraction file (Card NO. 09-432) which shows the typical hydroxyapatite patterns, and second phase was not detected. In Fig.1(b),

the broad diffuse peaks at  $19.5^\circ$  and  $40.8^\circ$  which corresponding to the characteristic peaks of PVA demonstrated that PVA possessed semi-crystalline structure<sup>[10]</sup>. Fig.1(c) presents the XRD pattern of *n*-HA/PVA composites which included characteristic peaks of both HA powder and PVA. It can be concluded from Fig.1 that HA powder can be synthesized effectively in PVA solution and *n*-HA/PVA gel composites can be prepared by *in situ* synthesis method.

Compared the characteristics peaks of HA in Fig.1(c) and Fig.1(a), it can be concluded that the intensity of characteristic peaks in Fig.1(c) are lowered and the shape of peaks broadened. According to Scherrer equation<sup>[12]</sup>, the crystallite size of HA particles can be determined as:

$$D_{(hkl)} = \frac{0.89\lambda}{\beta \cos\theta_{(hkl)}} \quad (2)$$

Where  $D$  is the average crystallite size,  $\beta$  the corrected full width of the peak at half of the maximum intensity,  $\lambda$  the wavelength of X-ray radiation, 0.89 is a constant related to the crystallite shape.

The crystallinity of HA can be calculated as follows<sup>[11]</sup>:

$$X_c = \left( \frac{0.24}{\beta} \right)^3 \quad (3)$$

It can be concluded from Equations (2) and (3) that both the crystallite size and crystallinity of HA synthesized in PVA solution decreased compared with that of HA synthesized in aqueous solution. The result corresponded with that of Nebahat<sup>[12]</sup>. This showed that PVA solution can effectively restrain the growth of HA grain and the aggregation of particles. Thus, it is beneficial to improve mechanical properties of the composites.

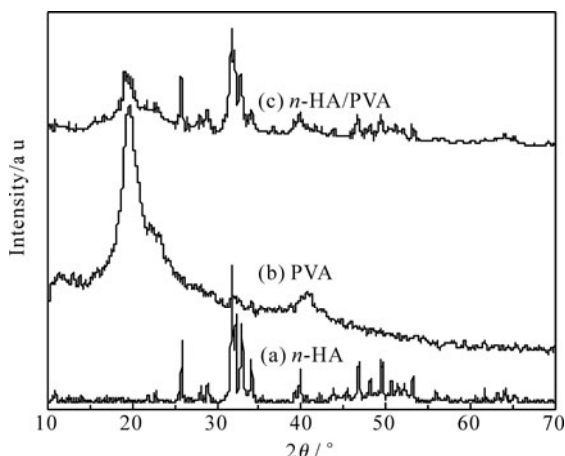
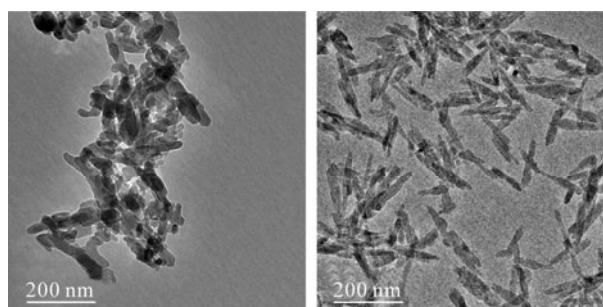


Fig.1 XRD pattern of the HA, PVA and *n*-HA/PVA gel composites

### 3.2 Microstructure of nano-HA and composites

Fig.2 shows the morphology of HA particles synthesized in aqueous solution and PVA solution, respectively, by TEM observation. It can be clearly seen that the crystalline grain of HA synthesized in this study is on the

nanometer scale. The morphology presents needle-like or rod-like shape with a diameter of 30 to 60 nm and length range 160 to 220 nm. There are some differences in morphology of HA prepared in two different solutions: (1) The ratio of length and diameter of HA particles synthesized in PVA solution is evidently larger than that of HA synthesized in aqueous solution. That is to say, the morphology of HA particles changed from rod-like in distilled water to needle-like in PVA solution. (2) The dispersion of HA particles in PVA solution is more homogenized than that in aqueous solution. The observed result of TEM is accordance with that of XRD.



(a) Aqueous solution (b) PVA solution

Fig.2 TEM morphology of HA particles synthesized in different solutions

Liu<sup>[13]</sup> has investigated the effect of PEG and cetylrimethyl ammonium bromide (CTAB) as dispersants on the morphology of HA particles. The results also showed needle-like structure of HA particle in the presence of CTAB and PEG. The effect of CTAB and PEG on the formation of HAp was attributed to the follows: (1) PEG is a non-ionic surfactant. The PEG monomer can easily form long chain structures in aqueous solution. (2) In an aqueous system, CTAB would ionize completely and result in a cation with tetrahedral structure. (3) The phosphate anion is also a tetrahedral structure.

In our study, PVA molecule also holds long chain structure in aqueous solution and similar to that of PEG. From Fig.2, it is proposed that the PVA possesses the ability to control the crystal growth process as well as to prevent conglomeration of HA particles. Therefore, HA nano-particles may grow along the long chains of PEG and needle-like structures formed when  $\text{Ca}^{2+}$  ions meet  $\text{PO}_4^{3-}$  and  $\text{OH}^-$  ions. Hence, PVA may be used as a soft template in the synthesis of HA particles. The result of Niu<sup>[14]</sup> also shows that the organic dispersants such as PVA and PEG can effectively improve the purity of HA particles and are beneficial to the dispersibility of the particles.

Fig.3 shows the SEM images of PVA gel and nano-HA/PVA gel composites after vacuum freeze-dried for 24 h. Fig.3 shows that the microstructure of both the pure PVA gel and nano-HA/PVA gel composites exit

many micro-pores on the surface of the materials. This result indicates that PVA hydrogel and the composites possess similar micro-pore structure to that of nature articular cartilage. The micro-pore structure of the composites is beneficial to the growth of chondrocytes while it is used as artificial cartilage repairing material. For the nano-HA/PVA gel specimen (Fig.3(b), (c) and (d)), large number of HA particles were observed in the PVA matrix. HA particles disperse homogeneously in PVA matrix with low content of HA particles (Fig.3(b) and (c)). On the other hand, it shows a tendency to agglomerate with an increase of nano-HA content in PVA matrix (Fig.3(d)).

The inorganic nano-particles possess high surface energy and high specific surface area. With low content of HA particles in PVA matrix, the PVA solution can also be used as a dispersant to provide a uniform HA particle size distribution in the matrix and no agglomeration occurs. Thus, the interfacial bonding strength between particle and polymer matrix is expected to be improved effectively due to the high surface energy and specific surface area of nano-particles and further increases the mechanical properties of the composites. Contrarily, the nano-HA particles can easily agglomerate because of its high surface active energy, while the content of nano-HA exceeding a certain percent. Therefore, both the specific surface and active sites on the surface of particles decrease greatly due to their agglomeration. At this time, the agglomeration of nano-HA particles cannot act as a reinforcement phase but becoming the original defective region which deteriorates the tensile strength of the composites.

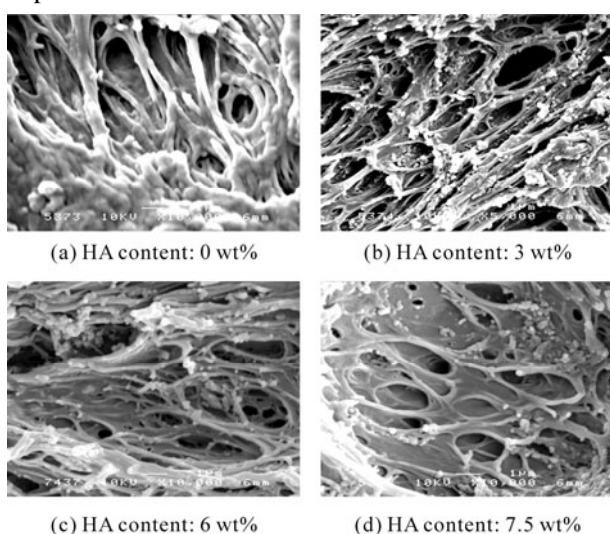


Fig.3 SEM images of the composites with various weight ratio of HA particles

### 3.3 IR analysis

Fig.4(a)-(c) indicates the FTIR spectra of HA, PVA and HA/PVA composites, respectively. The infrared band positions and their assignments are summarized in

Table 1. In the IR spectra of HA and HA/PVA composites, broad bands at  $3\ 500\text{--}3\ 400\ \text{cm}^{-1}$  and  $1\ 618\ \text{cm}^{-1}$  is an indicative of strongly adsorbed and/or bound water in the materials<sup>[13,15]</sup>. In Fig.4(a), absorption peaks at 882, 1 421 and 1 460  $\text{cm}^{-1}$  for carbonate ions have not been observed in the as-made materials<sup>[14]</sup>. This observation indicates that the prepared materials are only composed of HA particles. The strongest peak at  $1\ 033\ \text{cm}^{-1}$  and bands at 565 and 603  $\text{cm}^{-1}$  are attributed to the bending vibration of  $\text{PO}_4^{3-}$ . The band at 962  $\text{cm}^{-1}$  is belong to the stretching vibration of  $\text{PO}_4^{3-}$  and the band (bending) due to structural OH in HA also occurs at around 632  $\text{cm}^{-1}$ . In Fig.5(b), the band at 2 949  $\text{cm}^{-1}$  and 831  $\text{cm}^{-1}$  are attributed to the asymmetric stretching vibration and 1 384  $\text{cm}^{-1}$  belongs to the asymmetric bending vibration of  $-\text{CH}_2-$  group in PVA molecule. The stretching vibration of C-O is located at 1 095  $\text{cm}^{-1}$ <sup>[16]</sup>. It can be obviously seen from Fig.4(c) that the vibration bands of each functional group in HA and PVA molecule recurred in the vibration bands of HA/PVA composites.

It can be seen from Fig.4(b) and Fig.4(c), the vibration band positions of each functional group in PVA molecule tends to shift from high frequency to low frequency in HA/PVA composites while compared with that of pure PVA gel. For example, the asymmetric stretching and bending vibration bands of  $-\text{CH}_2-$  group shifted from 2 949 and 831  $\text{cm}^{-1}$  in pure PVA to 2 943 and 828  $\text{cm}^{-1}$  in HA/PVA composites, respectively. The stretching band of C-O group changed from 1 095  $\text{cm}^{-1}$  to 1 094  $\text{cm}^{-1}$  and the band of OH drifted from 1 618 to 1 616  $\text{cm}^{-1}$ , respectively, while HA particles was added into the PVA. The results of IR results indicate that the addition of HA particles has obvious effects on the structure of PVA molecule. The study of Chang *et al*<sup>[17,18]</sup> revealed that the calcium cation in HA and hydroxyl group in PVA molecule can form chemical bonding by the terms of  $[\text{HO-}]\text{Ca}^{2+}\text{-}[\text{OH}]$  linkage. The hydroxyl ion in the PVA

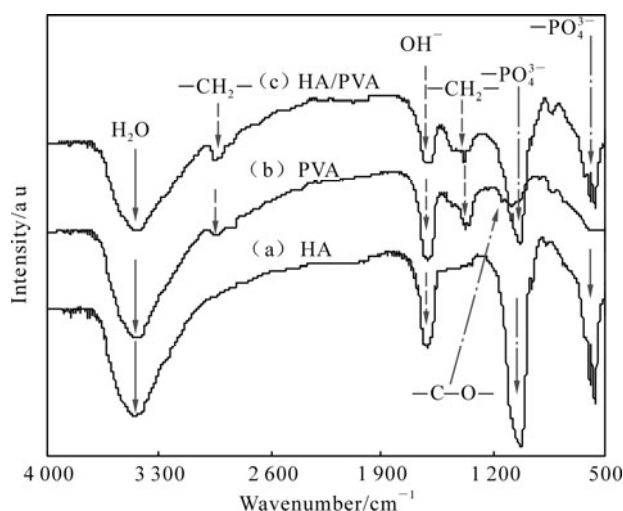


Fig.4 FTIR spectra of HA, PVA and HA/PVA composites

can be an especially active site for the complexation of the calcium ions in the HA which causes the OH group of PVA molecule to move towards the low frequency point. Furthermore, the conformation and degree of tacticity of PVA molecule changed due to the hydrogen bond interaction between HA and PVA molecule. This causes all the vibration band positions in PVA molecule changing from high frequency to low frequency.

**Table 1 Assignments of the observed vibration frequencies of HA, PVA and HA/PVA composites**

Assignments	Observed vibration frequencies/cm <sup>-1</sup>		
	PVA	HA	HA/PVA
H <sub>2</sub> O absorbed	—	3 448	3 442
Structural OH <sup>-</sup>	3 423	—	3 442.5
-CH <sub>2</sub> <sup>-</sup> asymmetric stretch	2 949,831	—	2 943,828
-CH <sub>2</sub> <sup>-</sup> asymmetric bend	1 384	—	1 380
-C-O <sup>-</sup> stretch	1 095	—	1 094
H <sub>2</sub> O absorbed (ν <sub>2</sub> )	—	1 618	1 618
PO <sub>4</sub> <sup>3-</sup> bend ν <sub>3</sub>	—	1 033	1 033
PO <sub>4</sub> <sup>3-</sup> stretch ν <sub>1</sub>	—	962	962
Structural OH <sup>-</sup>	1 618	632	1 616,630
PO <sub>4</sub> <sup>3-</sup> bend ν <sub>4</sub>	—	603	603
PO <sub>4</sub> <sup>3-</sup> bend ν <sub>4</sub>	—	565	565

## 4 Conclusions

a) The *n*-HA/PVA gel composites were prepared by *in situ* synthesis method and incorporation with freeze-thaw cycle process. XRD and TEM studies confirmed that the size of HA synthesized in PVA and aqueous solutions is on the nanometer scale. Both the crystallite size and crystallinity decreased in PVA solution compared with that of HA synthesized in aqueous solution.

b) In the synthesis of HA/PVA composites, PVA solution not only acts as matrix, but also as a dispersant. It is beneficial for the PVA solution to make HA particles distribute uniformly in PVA matrix. The HA particles trend to aggregate while the HA contents extend to a certain degree in PVA matrix.

c) FTIR study revealed that the interaction between the HA particle and PVA molecule existed and therefore the conformation and degree of tacticity of PVA molecule changed.

## References

- [1] Rebecca J C, Ott R D, David N K. Friction Characteristics of a Potential Articular Cartilage Biomaterial[J]. *Wear*, 2003 (25): 1 064-1 068
- [2] Shigo M, Katsuko S F, Takashi U, et al. Static and Dynamical Mechanical Properties of Extracellular Matrix Synthesized by Cultured Chondrocytes[J]. *Mater. Sci. Eng. C*, 2004(24): 425-429
- [3] Karen J L B, Scott P, James F K. Biomaterial Developments for Bone Tissue Engineering[J]. *Biomaterials*, 2000 (21): 2 347-2 359
- [4] Pan Y S, Xiong D S, Chen X L. Friction Characteristics of Poly (Vinyl Alcohol) Hydrogel as an Articular Cartilage Biomaterial[J]. *Key Eng. Mater.*, 2007 (330-332): 1 297-1 300
- [5] Noguchi T, Yamamuro T, Oka M. Poly (Vinyl Alcohol) Hydrogel as an Artificial Articular Cartilage: Evaluation of Biocompatibility[J]. *Appl. Biomaterials*, 1991, 2(2): 101-107
- [6] Pan Y S, Xiong D S. Recent Development on Biotribology of Poly (Vinyl Alcohol) Hydrogel[J]. *Tribology*, 2006, 26(2): 188-192 (in Chinese)
- [7] Suciu A N, Iwatsubo T, Matsuda M. A Study upon Durability of the Artificial Knee Joint with PVA Hydrogel Cartilage[J]. *JSME, Part C*, 2004, 47(1): 199-208
- [8] Stammen J A, Williams S, Ku D N. Mechanical Properties of a Novel PVA Hydrogel in Shear and Unconfined Compression[J]. *Biomaterials*, 2001 (22): 799-806
- [9] Ahn E S, Gleason N J, Nakahira A. Nanostructure Processing of Hydroxyapatite-based Bioceramics[J]. *Nano Letter*, 2001, 1(3): 149-153
- [10] Rosa R, Finizia A, Claudio D R, et al. X-ray Diffraction Analysis of Poly (Vinyl Alcohol) Hydrogels, Obtained by Freezing and Thawing Techniques[J]. *Macromolecules*, 2004 (37): 1 921-1 927
- [11] Rusu V M, Ng C H, Wilke M, et al. Size-controlled Hydroxyapatite Nanoparticles as Self-organized Organic-inorganic Composite Materials[J]. *Biomaterials*, 2005 (26): 5 414-5 426
- [12] Nebahat D, Dilhan M K, Elvan B. Biocomposites of Nano-hydroxyapatite with Collagen and Poly (Vinyl Alcohol)[J]. *Colloids and Surfaces B: Biointerfaces*, 2006 (48): 42-49
- [13] Liu Y K, Houm D D, Wang G H. A Simple Wet Chemical Synthesis and Characterization of Hydroxyapatite Nanorods[J]. *Mater. Chem. Phys.*, 2004 (86): 69-73
- [14] Niu L T, Liu J X, Zhou J, et al. Preparation and Characterization of Hydroxyapatite Extra-fine Powder by Using Polyvinyl Alcohol as Organic Modifier[J]. *Dalian Institute of Light Industry*, 2004, 23(4): 239-241(in Chinese)
- [15] Sahai N, Tossell J A. Molecular Orbital Study of Apatite (Ca<sub>5</sub>(PO<sub>4</sub>)<sub>3</sub>OH) Nucleation at Silica Bioceramic Surfaces[J]. *Phys. Chem. B*, 2000, 104(18): 4 322-4 341
- [16] Suprabha N, Arvind S. Systematic Evolution of a Porous Hydroxyapatite-Poly(vinylalcohol)-Gelatin Composite [J]. *Colloids and surfaces B: Biointerfaces*, 2004 (35): 29-32
- [17] Chang M C, Tanaka J. FT-IR Study for Hydroxyapatite/Collagen Nanocomposites Cross-linked by Glutaraldehyde[J]. *Biomaterials*, 2002 (23): 4 811-4 818
- [18] Chang M C, Ko C C, Douglas W H. Preparation of Hydroxyapatite-Gelatin Nanocomposites[J]. *Biomaterials*, 2003, 24(17): 2 853-2 862